JOURNAL OF GEOPHYSICAL RESEARCH, VOL. 103, NO. A9, PAGES 20,481-20,486, SEPTEMBER 1, 1998

Effect of heavy ions on ponderomotive forces due to ion cyclotron waves

F. Z. Feygin, O. A. Pokhotelov, and D. O. Pokhotelov

Institute of Physics of the Earth, Moscow, Russia

K. Mursula, J. Kangas,[1] T. Bräysy, and R. Kerttula

Department of Physical Sciences, University of Oulu, Oulu, Finland

Abstract. We study ponderomotive effects induced by the electromagnetic ion cyclotron (EMIC) waves in the Pc1 frequency band (0.2 to 5.0 Hz) in a two–ion (H^+ and one heavy ion, e.g., He^+) plasma. Near the dayside boundary of the magnetosphere, the ponderomotive forces lead to a noticeable accumulation of cold plasma along the field line in two regions of minimum magnetic field intensity located symmetrically around the equator. In the inner magnetosphere, one maximum of cold plasma at the equator is found. At frequencies less than the heavy ion gyrofrequency, the accumulation of cold plasma increases with increasing heavy ion concentration. At frequencies above the heavy ion gyrofrequency, the ponderomotive forces due to EMIC waves are enhanced because of a resonance at the stop band frequencies. We investigate the stop band structure of EMIC waves in a nondipolar magnetosphere and discuss the properties of wave propagation along the field line for different heavy ion plasma concentrations.

1. Introduction

Considerable attention has been paid to study the influence of heavy ions (mainly oxygen and helium) on the dynamics of electromagnetic ion cyclotron waves in the Pc1 frequency range (0.2 to 5.0 Hz). Using the search–coil magnetometer and particle spectrometer data onboard GEOS 1 and ATS 6 satellites, *Young et al.* [1981] and *Mauk et al.* [1981] came to the conclusion that EMIC waves are strongly controlled by the dynamics of heavy ions. Later on, *Fraser et al.* [1986] obtained similar results using ISEE 1 and 2 data.

The propagation of EMIC waves along magnetic field lines in a heavy ion rich plasma is characterized by the reversal of polarization and the splitting of spectrum into two branches, the high-frequency branch $\omega > \Omega_i$ (Ω_i stands for the heavy ion gyrofrequency) and the low-frequency branch $\omega < \Omega_i$. The two branches are separated by a stop band whose width is roughly $\triangle\omega = \Omega_i(N_i/N)[(m_i/m_p)-1]$. Here m_p and m_i stand for proton and heavy ion masses, respectively, and N is the total plasma density ($N = N_e = N_p + N_i$). Observations onboard the GEOS 1, 2 satellites [*Young et al.*, 1981] have shown that EMIC wave spectra are concentrated in the vicinity of the equatorial He^+ gyrofrequency. These observations also showed that there is an inverse connection between increases in He^+ concentration and the occurrence of Pc1 events on ground, thus verifying the important role of He^+ ions for the generation and propagation of EMIC waves.

It is well known by now that ponderomotive forces induced by EMIC waves can significantly affect the plasma balance in the Earth's magnetosphere [see, e.g., *Allan*, 1992, 1994; *Guglielmi et al.*, 1995; *Guglielmi and Pokhotelov*, 1996; *Witt et al.*, 1995; *Pokhotelov et al.*, 1996]. It was demonstrated that if the amplitude of EMIC waves exceeds a certain critical value, a pronounced maximum of plasma density is formed in the vicinity of minimum magnetic field intensity along the wave trajectory. *Pokhotelov et al.* [1996] studied ponderomotive forces near the dayside magnetospheric boundary, where the geomagnetic field changes, when moving radially outward, from a V-type structure with one intensity minimum to a W-type structure with two minima (so called magnetic holes) along the field line. They showed that the ponderomotive forces can lead to a plasma accumulation in the vicinity of these magnetic holes. On the other hand, *Feygin et al.* [1997] studied the ponderomotive forces at different magnetic local times and showed that when moving away from the noon meridional plane close to the dayside boundary, the plasma density distribution along the field

[1]Now at Geophysical Observatory, Sodankylä, Finland.

Paper number 98JA01903.
0148-0227/98/98JA-01903$09.00

line varies from two off-equatorial maxima at noon to one equatorial maximum outside the noon. They also proposed that the ponderomotive forces due to EMIC waves may form high-density plasma clouds far outside the plasmasphere, similar to the regions of detached plasma.

In all studies mentioned above the effects of ponderomotive forces have been treated by assuming one ion species (H^+) only. The present study is the first to investigate the effects of ponderomotive forces in a plasma including heavy ions. In the following section the relevant theoretical formulation is presented, assuming one heavy ion species in addition to H^+ ions. This assumption is valid, for example, during quiet geomagnetic conditions when the effect of He^+ ions is important but the heavier ions can be neglected. In section 3 we estimate some of these results numerically. We discuss the ponderomotive forces and wave propagation in a nondipolar magnetic field in section 4. Finally, section 5 presents our conclusions.

2. Basic Equations

Similarly to *Pokhotelov et al.* [1996], our analysis is based on the analytical model of the Earth's magnetic field presented by *Antonova and Shabanskii* [1968]. This model was shown by *Antonova et al.* [1983] to be in good agreement with magnetic field observations by the HEOS 1 and 2 satellites in the dayside magnetosphere. According to this model the geomagnetic field is modeled by a superposition of two dipoles: the internal dipole with magnetic moment M and an additional dipole with magnetic moment kM. The latter dipole models the distortion of the dipole magnetic field caused by the solar wind pressure.

In a spherical coordinate system, the magnetic field components of this model can be written in the following form:

$$B_r = -\frac{\partial U}{\partial r}, B_\Theta = -\frac{1}{r}\frac{\partial U}{\partial \Theta}, B_\lambda = -\frac{1}{r\sin\Theta}\frac{\partial U}{\partial \lambda}, U = U_1 + U_2, \quad (1)$$

$$U_1 = -\frac{B_0}{r^2}\cos\Theta, \quad (2)$$

$$U_2 = \frac{kB_0 r\cos\Theta}{(r^2 + a^2 - 2ar\sin\Theta\cos\lambda)^{3/2}}, \quad (3)$$

where r is the geocentric distance (in Earth radii, R_E), a is the distance between the internal and additional dipole, Θ is the polar angle, λ is the geomagnetic longitude measured from the line connecting the two dipoles ($\lambda = 0^0$ is the local noon), and $B_0 = 3 \times 10^{-5}$T is the equatorial magnetic field intensity at the Earth's surface.

Magnetic field lines are determined by

$$\frac{\partial r}{\partial s} = \frac{B_r}{B}, \frac{\partial \Theta}{\partial s} = \frac{1}{r}\frac{B_\Theta}{B}, \frac{\partial \lambda}{\partial s} = \frac{1}{r\sin\Theta}\frac{B_\lambda}{B}, \quad (4)$$

where ∂s stands for the field line element. Below we will use the values $a = 33$ and $k = 13$, which locate the magnetospheric boundary in the noon meridional plane at 10 R_E. (The axes of the two dipoles are assumed to be parallel to each other.) In the outer dayside magnetosphere close to noon, the magnetic field intensity along the field line has two minima located symmetrically with respect to the equator. When moving away from the noon meridional plane, the influence of the additional dipole which models the action of the solar wind becomes weaker and the two minima smoothly transform to one equatorial minimum.

Now let us consider the action of the ponderomotive forces induced by EMIC waves propagating along the magnetic field lines. Nonlinear interaction of large-amplitude EMIC waves with background plasma in a magnetic field having significant spatial gradients leads to the appearance of an electromagnetic force called the ponderomotive force. The field-aligned component of this force has the following form [*Guglielmi et al.*, 1993; *Guglielmi and Pokhotelov*, 1996]:

$$f_\parallel = \frac{1}{4\mu_0 c^2}[E^*_\alpha E_\beta \frac{\partial \varepsilon_{\alpha\beta}}{\partial B_\gamma}\nabla_\parallel B_\gamma + (\varepsilon_{\alpha\beta} - \delta_{\alpha\beta})\nabla_\parallel E^*_\alpha E_\beta] \quad (5)$$

where $E = (1/2)[E^0\exp(-i\omega t) + E^{*0}\exp(i\omega t)]$ is the wave electric field, $\varepsilon_{\alpha\beta}$ is the dielectric permittivity tensor, $\delta_{\alpha\beta}$ is the Kronecker symbol, c is the speed of light, and μ_0 is the permeability of free space. (In the following the superscript 0 will be omitted from E.)

The terms on the right-hand side of (5) refer to the field-aligned components of Pitaevskii force and Miller force, respectively [see, e.g., *Guglielmi and Pokhotelov*, 1996]. In the following, we will rearrange (5) using the relation $b = nE/c$, where b is the wave magnetic field, n is the refraction index, and c is the speed of light. E, B, and n are evaluated at the equatorial crossing of the field line. Moreover, we use the relation $E \sim (B/n)^{1/2}$, which is a simple consequence of Faraday's law and the energy flux conservation.

We consider a plasma which consists of electrons, protons and one heavy ion species. The refractive index for left-hand circularly polarized electromagnetic waves in such a two–ion plasma is given by [see, e.g., *Guglielmi and Pokhotelov*, 1996]:

$$n^2 = 1 + \frac{\omega_{pp}^2}{\Omega_p(\Omega_p - \omega)} + \frac{N_i}{N_p}\frac{\omega_{pp}^2}{\Omega_p(\Omega_i - \omega)} \quad (6)$$

where ω_{pp} is the proton plasma frequency. The operator $\nabla_\parallel$ in (5) can be replaced by $(1/R_E)(dx/ds)d/dx$ where the field line element is given as follows:

$$ds = [r^2/(1-x^2) + (dr/dx)^2 + r^2(1-x^2)(d\lambda/dx)^2]^{1/2}dx \quad (7)$$

and $x = \sin(90^0 - \Theta)$.

Taking into account the above expressions we may now rewrite the field-aligned component of the ponderomotive force (5) as follows:

$$f_{\parallel} = -\frac{b_0^2}{4\mu_0 c^2 P^{1/2} R_E}\left(\frac{1}{\alpha\alpha_0}\right)^{1/2}\left(\frac{1-\nu_{p0}}{1-\nu_p}\right)^{1/2} \times \left\{\left[\frac{\nu_p(1-\nu_i)^2+(I/P)\nu_i(1-\nu_p)^2}{(1-\nu_p)(1-\nu_i)^2}\right] P\nabla_x \ln B + \nabla_x P + \frac{(1-\nu_p)}{(1-\nu_i)}\nabla_x I\right\}\frac{dx}{ds} \quad (8)$$

where $P = \rho_p/\rho_{p0}$, $I = \rho_i/\rho_{p0}$, ρ stands for plasma mass density, $\alpha = 1 + (I/P)(1-\nu_p)/(1-\nu_i)$, and $\nu = \omega/\Omega$. Subscript 0 refers to values close to the equator. Subscripts p and i correspond to proton and heavy ion, respectively. For $I = 0$ the expression (8) reduces to the well-known equation for a single-ion plasma [see, e.g., *Feygin et al.*, 1997].

The equation of plasma force balance in the field-aligned direction takes the form

$$\nabla_{\parallel}\rho c_s^2 = \rho g_{\parallel} + f_{\parallel} \quad (9)$$

where $\rho = \rho_p + \rho_i = N_p m_p + N_i m_i$, $c_s = (T_{eff}/m)^{1/2}$, $m = (m_p+m_i)/2$ and $T_{eff} = (N_h T_h + N_c T_c)/(N_h+N_c)$, where subscripts h and c refer to the hot and cold plasmas, respectively. T is plasma temperature. Finally, the field-aligned component of the gravity force is

$$g_{\parallel} = \frac{B_r}{B}\frac{g_E}{r^2} \quad (10)$$

where $g_E = 9.8$ m/s^2 and B_r and B are defined by the relations (1)–(3). Substituting (8) and (10) into (9) we find the following first-order differential equation which determines the distribution of plasma density along the field line in a two-ion plasma:

$$P^{1/2}\nabla_x(P+I) + A_3[\nabla_x P + \frac{(1-\nu_p)}{(1-\nu_i)}\nabla_x I] = A_1 P^{1/2}(P+I) + A_2 P[1 + \frac{I}{P}\frac{\nu_i}{\nu_p}\frac{(1-\nu_p)^2}{(1-\nu_i)^2}] \quad (11)$$

where

$$A_1 = \frac{g_{\parallel}}{c_s^2}\frac{ds}{dx}R_E \quad (12)$$

$$A_2 = -A_3\frac{\nu_p}{(1-\nu_p)}\nabla_x \ln B \quad (13)$$

$$A_3 = \frac{b_0^2}{4\mu_0 c^2}\frac{1}{(\alpha\alpha_0)^{1/2}}\frac{1}{\rho_0 c_s^2}\left(\frac{1-\nu_{p0}}{1-\nu_p}\right)^{1/2}. \quad (14)$$

3. Numerical Analysis

We have integrated (11) using the Runge-Kutta method and the boundary condition $P = 1$ at $x = 0$. Figure 1 displays the location of the density maxima at different L shells for a pure proton plasma (I=0) (a) in the noon meridional and (b) in the off-noon meridional plane ($\lambda = 20^0$). We have taken the square of the sound velocity $c_s^2 = 5 \times 10^8$ m^2/s^2, the plasma mass density at the equator $\rho_0 = 1.67 \times 10^{-20}$ kg/m^3, $\nu_{p_0} = 0.2$, and $b_0 = 5$ nT. It should be noted that the bifurcation starts closer to the Earth in the noon meridional plane than away from it. Moreover, the transition from the case of one equatorial density maximum to two off-equatorial maxima occurs more sharply in Figure 1b. These effects are connected with the weaker influence of the solar wind pressure outside the noon meridional plane.

Figure 2 depicts the distribution of normalized proton density along the field line for different values of I_m, the normalized heavy ion density averaged over the field line. Other parameters are $c_s^2 = 5 \times 10^8$ m^2/s^2, $\rho_0 = 1.67 \times 10^{-20}$ kg/m^3, $\nu_{p_0} = 0.2$, $b_0 = 5$ nT, and $\lambda = 0^0$. Figure 2a corresponds to $L = 6$ and Figure 2b to $L = 9.5$. Note that we have assumed here $\nu_{i_o} < 1$, whereby, together with the assumption $\nu_{p_0} = 0.2$, this case only applies for the case of He^+ ion. It is evident that as I_m is increased, the ponderomotive effect becomes more pronounced both at a lower L shell with one maximum

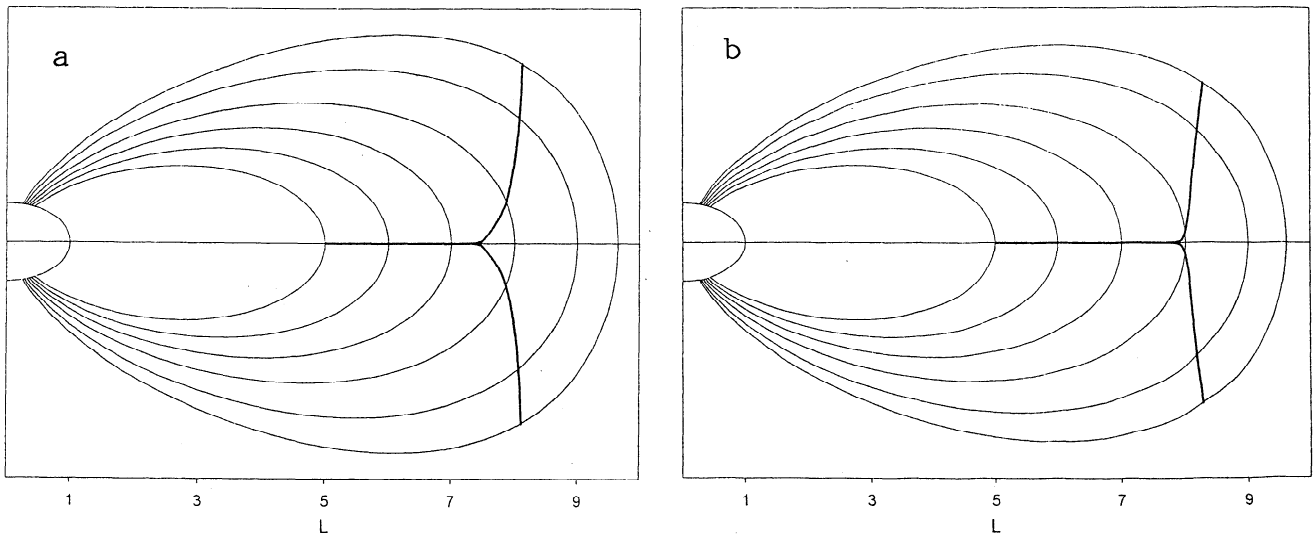

Figure 1. The position of the proton density maximum for different L shells in the absence of heavy ions (I=0) (a) in the noon meridional plane ($\lambda = 0^0$), and (b) at the longitude $\lambda = 20^0$.

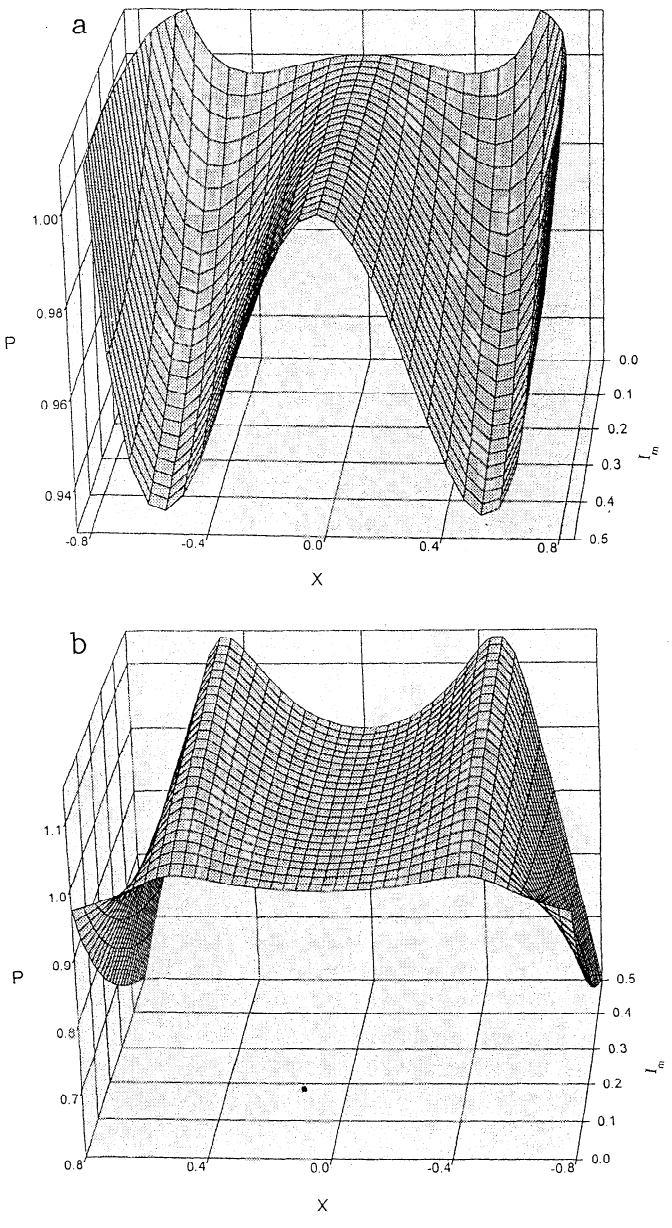

Figure 2. The normalized proton density along the field line as a function of $x = \sin(90^0 - \Theta)$ and the mean normalized helium density (I_m) at noon ($\lambda = 0^0$) in the case of $\nu_i < 1$ at (a) $L = 6$ and (b) $L = 9.5$. (Note that the I_m axis runs in opposite direction in the two figures.)

(Figure 2a), as well as at a higher L shell with two maxima (Figure 2b).

The similar distribution of a normalized proton density in the case of He^+ ions with $\nu_{i_o} > 1$ ($\nu_{i_0} = 2.0$; $\nu_{p_0} = 0.5$) is depicted in Figure 3 for $L = 9$ using the same parameter values as above. Moreover, Figure 4 shows the distribution of normalized proton density as a function of L value, taking $I_m = 0.5$ and $\nu_{i_0} = 2.0$, and other parameters as in Figure 3. The case of $\nu_i > 1$ is more difficult for numerical analysis than the case of $\nu_i < 1$ because of the singularity $\alpha = 0$ in the denominator of (14).

4. Discussion

It was demonstrated above that heavy ions may significantly modify the action of ponderomotive forces. We have restricted ourselves in this paper to the case of one heavy ion only, with a particular attention to helium ions. Also, we only studied field-aligned propagation. It is well known that in cold plasma without heavy ions the L mode EMIC wave is guided while the R mode remains unguided. In the presence of heavy ions, the L mode exhibits resonant behavior near the helium gyrofrequency and the cutoff frequency. The latter one can be found from (6) to be $F_{cf_0} = \Omega_{He_0^+}(1+3\eta_0)$, where $\eta_0 = N_{He_0^+}/N_0$. The stop band is located between these two frequencies where the L mode is evanescent.

In a two-ion plasma studied here, the behavior of the ponderomotive force becomes complex. In particular, $f_\parallel$ also has resonances. In the dipole field model, the first resonance is at $\nu_1 = \nu_{i0} = 1$, and the second one is at $\nu_2 = \nu_{i0} = 1 + 3\eta_0 = 1 + 3I_0/(4 + I_0)$. Thus the ponderomotive forces in the equatorial region have the same stop band as for EMIC wave propagation. This is quite evident since the ponderomotive forces are induced by EMIC wave propagating along the field line. At large η_0, the width of the stop band increases, narrowing the propagation region of EMIC waves with $\nu_{i0} > 1$, and decreasing the plasma density accumulation compared to the case of $\nu_{i0} < 1$. For nonequatorial region in the case of $\nu > \nu_2$, the value α can also become a singularity. Therefore, at frequencies $\omega > F_{cf_0}$, the ponderomotive forces have a resonance (i.e., become infinite) at the following frequency:

$$\omega = F_{cfl} = \Omega_{He_l^+}(1 + 3\eta_l) \tag{15}$$

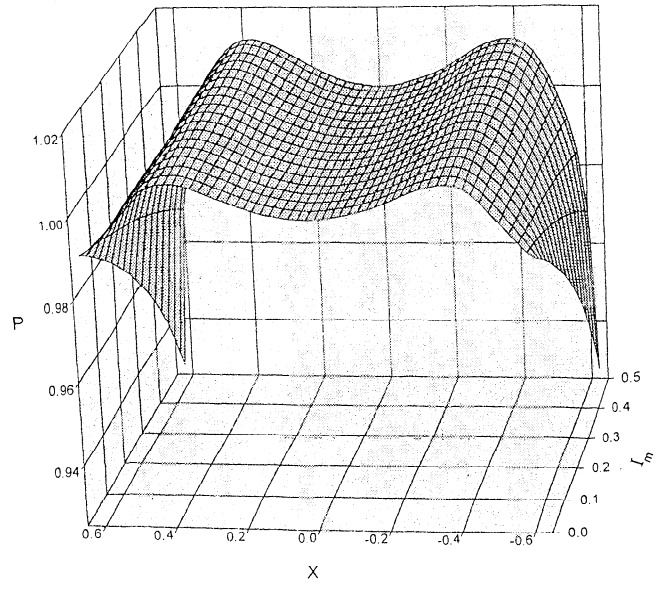

Figure 3. The same as in Figure 2 but for the case $\nu_i > 1$ ($\nu_{i_0} = 2.0$; $\nu_{p_0} = 0.5$) and $L = 9.0$.

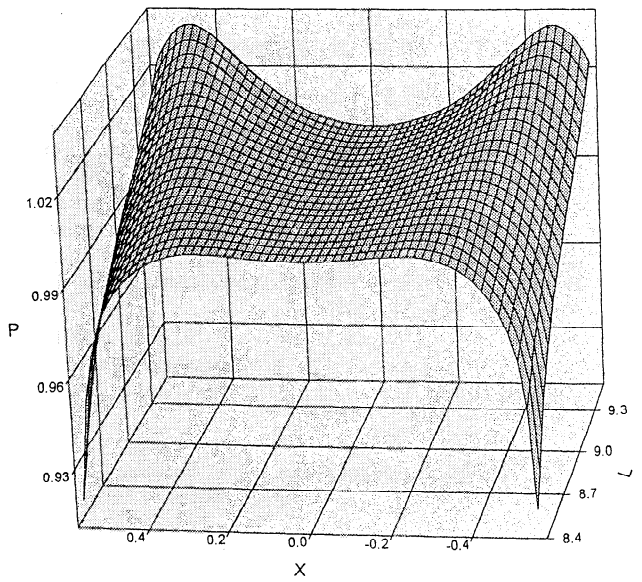

Figure 4. The normalized proton density along the field line as a function of $x = \sin(90^0 - \Theta)$ and L value at noon ($\lambda = 0^0$) for $I_m = 0.5$ and $\nu_i > 1$.

where $\eta_l = N_{He^+l}/N_l$, F_{cfl} is the local cutoff frequency (subscript l refers to local off-equatorial values). The value of the resonant frequency is determined by the plasma condition at each point on the field line, depending on the influence of ponderomotive forces. The analysis of the expression for the ponderomotive force in the two–ion plasma (8) shows that the largest values of the forces for $\omega > F_{cf_0}$ are not attained at the equator as found for single-ion plasma [*Guglielmi and Pokhotelov*, 1996] but close to the region where $\omega \approx F_{cfl}$.

Now let us discuss the problem of EMIC wave propagation along a nondipolar field line in a two-ion plasma, and the action of ponderomotive forces in such a plasma. As discussed above, the dayside geomagnetic field changes smoothly from a V-type structure with one intensity minimum to a W-type magnetic field structure with two intensity minima along the field line. One can analyze the dispersion equation (6) in such a field in a He^+-rich plasma using a schematic diagram of Figure 5 which displays the effects of wave propagation from equatorial region to higher magnetic latitudes at high L close to the noon.

In a nondipolar magnetosphere the stop band structure of EMIC waves differs from that of dipolar field lines (see Figure 5). In the dipolar magnetosphere, the minimum resonant frequency equals $\omega = \Omega_{He_0^+} = F_1$ while in the nondipolar magnetosphere the minimum resonant frequency is determined by $F_2 = \Omega_{He^+_{min}}$, where the minimum magnetic field in $\Omega_{He^+_{min}}$ is determined by (1)–(3). Thus only waves with frequencies $\omega < F_2$ can easily reach the Earth's surface. Therefore it is possible to suppose that EMIC waves with frequencies $F_2 < \omega < F_1$ exist in the near-equatorial region close to the dayside magnetospheric boundary, but can not propagate to the Earth's surface. Such an effect does not exist in the dipolar magnetic field, where all the waves with frequencies $\omega < F_1$ can propagate to the Earth's surface.

The conditions of EMIC wave propagation have a strong influence on the redistribution of plasma density along the field line. For $\omega > F_{cf_0}$, the effect of ponderomotive forces is enhanced when the stop band width becomes smaller, i.e., when η is decreased. This is connected with an extended EMIC wave propagation range and, correspondingly, with an extended range of the ponderomotive force which causes the denser plasma to move from lower altitudes along the field line to the magnetic field minimum. At very small values of η, the effect of thermal motion of heavy ions should also be taken into account. *Nekrasov* [1988] demonstrated that for typical magnetospheric parameters the helium ions having the energy of the order of a few eV do not form stop bands if their concentration is small, $\eta \leq 10^{-2}$. In this case, EMIC waves with frequencies which coincide with the helium gyrofrequency will propagate through the cyclotron resonance, partially losing energy.

5. Conclusion

We conclude by summarizing the main results obtained in this paper: (1) We have derived general formulas for the ponderomotive force induced by electromagnetic ion cyclotron waves in a plasma containing protons and one heavy ion species. (2) We have estimated the effect of the ponderomotive force during quiet

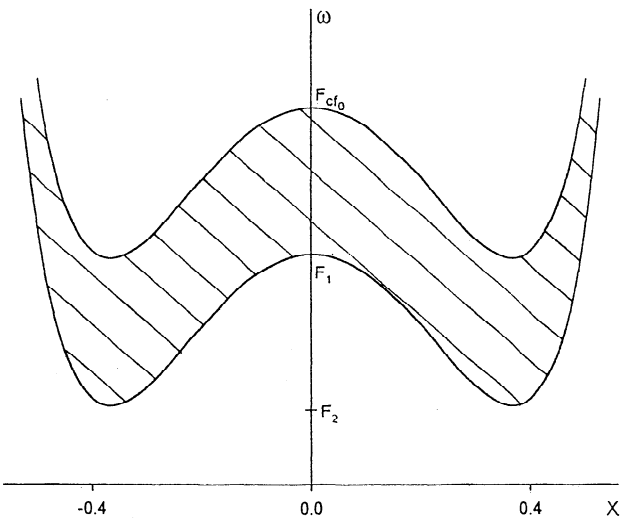

Figure 5. Schematic presentation of effects affecting wave propagation from the equator to higher geomagnetic latitudes in a nondipolar magnetosphere close to the dayside magnetospheric boundary. The shaded area corresponds to the the forbidden frequency band (stop band) for L mode EMIC waves due to heavy (e.g., helium) ions. F_1 is the equatorial helium gyrofrequency, F_{cf_0} is the equatorial cutoff frequency, and F_2 is local helium gyrofrequency in the region of minimum magnetic field intensity.

geomagnetic conditions when the helium ions are the dominant heavy ion species and affect the EMIC waves. (3) For frequencies less than the helium gyrofrequency, the ponderomotive force effects are increased with increasing concentration of helium ions. We verify the result obtained earlier for the case of no heavy ions that plasma is accumulated around the regions of minimum magnetic field intensity. Close to dayside boundary of the magnetosphere this leads to two density maxima located symmetrically with respect to the equator. (4) If the wave frequency approaches the boundary frequency of a stop band formed by the heavy ion, ponderomotive force has a singularity and may be greatly amplified. (5) We discuss the propagation of the L mode EMIC waves from the equatorial to higher magnetic latitudes in a nondipolar magnetic field. We note that in this case there is a range of frequencies below the equatorial helium gyrofrequency where the L mode can not propagate to Earth's surface. Accordingly, the ponderomotive forces can have a singularity both for frequencies above and below the equatorial helium gyrofrequency. This effect is missing in a dipolar magnetosphere.

Acknowledgments. This research was partially supported by the Academy of Finland, the INTAS organisation (grant 94-2811), the Russian Fund for Basic Research (grants 97-05-64606 and 97-05-65404), and the Ministry of Science and Technology of Russia (Upper Atmosphere Physics, Arctic and Antarctic Project). The authors are also grateful to A. V. Guglielmi for useful discussions.

The editor thanks David M. Walker and another referee for their assistance in evaluating this paper.

References

Allan W., Ponderomotive mass transport in the magnetosphere, *J. Geophys. Res., 97*, 8483, 1992.

Allan W., Time dependence of ponderomotive plasma energization in the magnetosphere, *J. Geophys. Res., 99*, 21281, 1994.

Antonova A. E., and V. P. Shabanskii, Structure of the geomagnetic field at great distances from the Earth, *Geomagn. Aeron., 8*, 639, 1968.

Antonova, A. E., V. P. Shabanskii, and P. C. Hedgecock, Comparison of the empirical model of the magnetic field based on the data of HEOS 1,2 with the analytical two-dipole model of the magnetosphere, *Geomagn. Aeron., 23*, 574, 1983.

Feygin, F. Z., O. A. Pokhotelov, D. O. Pokhotelov, T. Bräysy, J. Kangas and K. Mursula, Exo–plasmaspheric refilling due to ponderomotive forces induced by geomagnetic pulsations, *J. Geophys. Res., 102*, 4841, 1997.

Fraser, B. J., J. C. Samson, R. L. McPherron, and C. T. Russell, Ion cyclotron waves observed near the plasmapause, *Adv. Space Res., 6*, (3)223, 1986.

Guglielmi, A., and O. Pokhotelov, *Geoelectromagnetic Waves*, Adam Hilger, Bristol, 1996.

Guglielmi, A. V., O. A. Pokhotelov, L. Stenflo, and P. K. Shukla, Modifications of the magnenetospheric plasma due to ponderomotive forces, *Astrophys. Space Sci., 200*, 91–96, 1993.

Guglielmi, A. V., O. A. Pokhotelov, F. Z. Feygin, Yu. P. Kurchashov and J. F. McKenzie, P. K. Shukla, L. Stenflo, and A. S. Potapov, Ponderomotive forces in longitudinal MHD waveguides, *J. Geophys. Res., 100*, 7997, 1995.

Mauk, B. H., C. E. McIlwain, and R. L. McPherron, Helium cyclotron resonance within the Earth's magnetosphere, *Geophys. Res. Lett., 8*, 103, 1981.

Nekrasov, A. K., On absence of the stop bands in the multicomponent plasma, *Geomagn. Aeron., 28*, 164, 1988.

Pokhotelov, O. A., F. Z. Feygin, L. Stenflo, and P. K. Shukla, Density profile modifications by electromagnetic ion cyclotron wave pressures near the dayside magnetospheric boundary, *J. Geophys. Res., 101*, 10,827, 1996.

Witt, E., M. K. Hudson, X. Li., I. Roth, and M. Temerin, Ponderomotive effects on distributions of O^+ ions in the auroral zone, *J. Geophys. Res., 100*, 12,151, 1995.

Young, D. T., S. Perraut, A. Roux, C. de Villedary, R. Gendrin, A. Korth, G. Kremser, and D. Jones, Wave–particle interactions near Ω_{He+} observed on GEOS 1 and 2, 1, Propagation of ion cyclotron waves in He^+-rich plasma. *J. Geophys. Res., 86*, 6755, 1981.

T. Bräysy, R. Kerttula, and K. Mursula, Department of Physical Sciences, University of Oulu, FIN–90570 Oulu, Finland. (e-mail: timo.braysy@oulu.fi, kalevi.mursula@oulu.fi)

F. Z. Feygin, D. O. Pokhotelov, and O. A. Pokhotelov, Institute of Physics of the Earth, 123810 Moscow, Russia. (e-mail: pokh@iephys.msk.su)

J. Kangas, Geophysical Observatory, FIN–99600 Sodankylä, Finland. (e-mail: jorma.kangas@sgo.fi)

(Received August 18, 1997; revised December 30, 1997; accepted April 17, 1998 .)